JOURNAL OF CATALYSIS 131, 276–284 (1991)

Short- and Long-Range Promotion by Sodium Additive in $D_2 + CH_2{=}CH_2$ Reaction over Silica-Supported Platinum Catalysts

HIDEAKI YOSHITAKE[1] AND YASUHIRO IWASAWA[2]

Department of Chemistry, Faculty of Science, The University of Tokyo, Hongo, Bunkyo-ku, Tokyo 113, Japan

Received October 4, 1990; revised February 25, 1991

The mechanism of $D_2 + CH_2{=}CH_2$ reaction on $Na/Pt/SiO_2$ was investigated to characterize the reaction environment of Pt surface modified by Na additive in relation to SMSI and general promoter effects. The structural and electronic properties of $Na/Pt/SiO_2$ catalysts were studied by TEM, XPS, and hydrogen adsorption (H/M). The H/M for Pt/SiO_2 coincides with that calculated from the average particle size in TEM, whereas for $Na/Pt/SiO_2$ it was always smaller than that expected from TEM. The peak intensity of Pt $4f_{7/2}$ decreased by small amounts of Na additives and kept constant in the higher loadings. From these results, we estimated the saturation coverage of Na on Pt surface to be 0.2. The binding energy of Pt $4f_{7/2}$ changed as a function of Na loading in the range of $\chi(=$ Na/(Na + Pt)) from 0.16 to 0.86, due to a direct interaction ($\chi < 0.43$) and an indirect interaction ($\chi \geq 0.43$) through SiO_2 surface. The deuterogenation of ethene was enhanced by Na addition. The profile of the deuterogenation activity of $Na/Pt/SiO_2$ is explained by the location of Na and the direct/indirect electron transfer. π-Ethene and di-σ-ethene at the Pt surfaces were observed by FT–IR. The rate of ethane formation and the ν_{C-H} of di-σ-ethene were correlated with Pt $4f_{7/2}$ binding energy. On the other hand, the rate of ethene–hydrogen exchange reaction and ν_{C-H} of π-ethene were independent of Na loading.

The dual site model for the deuterogenation and hydrogen exchange in the $D_2 + CH_2{=}CH_2$ system is proposed; the former reaction proceeds at the bare metal sites through di-σ-ethene and the latter occurs at the periphery sites around Na_2O island on Pt particles through π-ethene.

INTRODUCTION

The promotion of metal catalysis by metal additives or supports has been studied extensively from practical points of view in industries as well as by chemical interests. For such promoted catalysts unique catalytic performance/phenomenon and the microscopic reaction feature induced by second elements have been observed (*1–3*).

Alkali metals may result in a considerable modification of metal surface, due to the alternation of surface electronic structure by charge transfer. It has been reported to reduce the strength of the adsorption of $CH_2{=}CH_2$ (*4–6*) and C_6H_6 (*7*) or to strengthen the adsorption of CO (*8, 9*) and NO (*10*). The activation energy of CO hydrogenation decreases in the presence of alkali–metal, which is related to a large red shift of C–O stretching frequency (*11*). In addition to the electronic modification of surface, several authors have pointed out short-range effects of additives on adsorbates experimentally (*12, 13*) or theoretically (*14, 15*).

Metal catalysis is a dynamic process at the surface including short- and long-range interaction between adsorbates and additives. It is necessary for the microscopic clarification of alkali–metal additive effect in catalysis to in-

[1] Present address: Department of Energy Engineering, Faculty of Engineering, Yokohama National University, Tokiwadai, Hodogaya-ku, Yokohama 240, Japan.

[2] To whom correspondence should be addressed.

0021-9517/91 $3.00

vestigate the reaction mechanism relating to surface structures reflecting the working state.

We have been studying the local environments of reaction sites and the reaction mechanism of hydrogenations on SMSI catalysts, Rh/Nb_2O_5 (*16*), Ir/Nb_2O_5 (*16, 17*), and Pt/Nb_2O_5 (*18*). On these SMSI catalysts the electronic modification of metal surfaces and the cooperative catalysis by two kinds of sites have been observed. The bare metal sites far from migrated suboxides (NbO_x; $x < 2.5$) on metal surface and the peripheral sites of NbO_x were distinguished from each other. In this article, we have investigated the mechanism of D_2-ethene reaction on Na-promoted Pt/SiO_2 catalysts to understand the microscopic surface states and the short- and long-range effects of Na additives in relation to the genesis of essential factors for catalysis.

METHOD

SiO_2-supported platinum catalysts were prepared by an incipient wetness method using aqueous solution of $H_2PtCl_6 \cdot 6H_2O$ (Soekawa Chemical Co.) or by coimpregnation with aqueous solution of Na_2CO_3 (Wako Pure Chemical Industries, 99.7%) and $H_2PtCl_6 \cdot 6H_2O$. The impregnated samples were subsequently dried for 3 h at 393 K and calcined for 2 h at 773 K in air. Commercially available SiO_2 (Nippon Aerosil, ox-50, surface area: 50 $m^2 \cdot g^{-1}$) was used as support. The loading of platinum was always 2.4 wt%. Five kinds of $Na/Pt/SiO_2$ catalysts were prepared with varying amounts of sodium; 0.16, 0.43, 0.60, 0.70, or 0.86 in atomic molar ratio, χ = Na/(Na + Pt). These are equivalent to 0.19 to 6.1 times of Pt in atomic ratio. The catalysts thus obtained were placed in a closed circulating system that can be evacuated below 10^{-4} Pa. They were then treated with oxygen at 473 K for 1 h, followed by evacuation for 30 min, and reduced by hydrogen at 473 K for 1 h, followed by evacuation for 30 min before each catalytic reaction. These pretreatments cannot expel the significant amount of sodium from silica surface (*19*). Chlorine was not observed with all samples used by XPS in the wide scan mode. Hydrogen adsorption at 293 K was also carried out in this system.

We also prepared a Na-promoted catalyst of $\chi = 0.60$ by a two-step impregnation method. SiO_2 was impregnated with aqueous Na_2CO_3 solution, Na-doped dried for 3 h at 393 K, and calcined for 2 h at 673 K in air. The Na-doped support thus obtained was again impregnated with aqueous solution of $H_2PtCl_6 \cdot 6H_2O$. The following procedure was similar to that for coimpregnation samples. This $Pt/Na \cdot SiO_2$ catalyst gave the same results in the experiments, such as H/M, transmission electron microscopy (TEM), and D_2-$CH_2{=}CH_2$ reaction, as those for $Na/Pt/SiO_2$ with $\chi = 0.60$.

The particle size of platinum metal in the catalysts was determined by TEM. The electronic states of elements and surface composition in the catalysts were examined by XPS (Shimazu, ESCA 750). The absence of chlorine, sulfur, and the other poisoning elements was confirmed in wide scan mode.

Ethene (Takachiho Trading Co., 99.9%) was further purified by freeze–thaw cycles before each catalytic reaction. Hydrogen and deuterium gases of research grade were purified through a 5A molecular-sieve trap at 77 K.

The products of reactions were analyzed by gas chromatography with a TCD or by mass spectrometer (ANELVA AQA-100R operating with 70-eV electrons) after the separation by a 2-m VZ-10 column at 343 K. The usual corrections were made for natural isotopes (^{13}C and ^{12}C). The other corrections were small enough to be neglected.

The adsorbates on the catalysts were observed by IR (JASCO FT/IR–7000 with 2 cm^{-1} resolution). The catalysts were molded into self-supporting disks and mounted in the cell, which can be heated to 773 K. The IR cell was combined in the closed circulating system mentioned above.

TABLE 1

Dispersion and Particle Size of Platinum in the Catalysts

χ[a]	H/M	TEM (/nm)[b]	Na coverage[c]
0.00	0.31	4.1 (0.30)	0
0.16	0.24	5.5 (0.22)	0.1
0.43	0.13	8.0 (0.16)	0.2
0.60	0.13	8.0 (0.16)	0.2
0.70	0.13	7.8 (0.17)	0.2
0.86	0.13	7.9 (0.16)	0.2

[a] χ = Na/(Na + Pt).

[b] The values in the parentheses are the estimated dispersion by TEM after Anderson (*20*).

[c] Calculated from the results of H/M and TEM.

RESULTS AND DISCUSSION

(*i*) *The Structure and Electronic State of the Catalyst Surface*

The average particle size estimated by TEM and the dispersion determined by hydrogen adsorption (H/M) are summarized in Table 1. The dispersion expected from the particle size of TEM (*20*) was smaller than the value of H/M in the case of the presence of Na, assuming that one H atom corresponded to one surface Pt atom and Pt particles are spherical. The comparison of Pt dispersion evaluated by two different experiments would be valid to some extent because both values of dispersion from H/M and TEM are almost the same in the unpromoted catalyst. Since hydrogen is not adsorbed on sodium at room temperature, the surface ratio of Na to Pt, coverage θ_{Na}, can be evaluated from the difference in the dispersion calculated by H_2 adsorption and TEM. The results of the estimation are listed in the last column of Table 1.

The degree of error in the dispersion calculated from TEM should be described because the size of the Pt particles on the SiO_2 (ox-50) are usually distributed, involving smaller and larger particles. The Pt particle sizes were distributed relatively uniformly as illustrated in TEM photographs of Fig. 1. The deviation from the average particle size is estimated to be ± 1.2 nm. Accordingly, the error of Na coverage in Table 1 was evaluated to be ± 0.1. Nevertheless, it is to be noted that the values of Na coverage are the averaged values for Pt particles contained in each catalyst.

Pt particle size distributions in Na/Pt/SiO_2 catalysts in the range $0.43 \leq \chi \leq 0.86$ were very similar. The surface coverage θ_{Na} was constant at 0.2. In the catalyst with $\chi = 0.16$ Pt particles are thought to be in a mixed state of Pt particles with and without Na.

Table 2 shows the results of XP spectra, in which the binding energies and peak intensities of Pt $4f_{7/2}$ level are listed. The binding energy decreased by the loading of Na and continuously decreased with an increase of Na quantity. The intensity also decreased by Na loading but was constant from $\chi = 0.43$. Since the particle size was almost the same in the range of more than $\chi = 0.43$, the shift of the binding energy may result from the electron donation from Na to Pt rather than extra-atomic relaxation or particle size effect. The peak intensities of Pt (I_{Pt}) and Na (I_{Na}) as a function of Na loading are plotted in Fig. 2, where I_{Pt} was normalized by H/M due to surface area calibration. I_{Pt} was constant in $\chi \geq 0.43$, which is consistent with the constant coverage of Na on Pt particle in Table 1. I_{Pt} for $\chi = 0.16$ was similar to I_{Pt} for the samples with $\chi \geq 0.43$. This may indicate that Na cluster/particles with a similar size start to cover the Pt particle surfaces from a low content of Na.

On the other hand, I_{Na} increased monotonously, showing an upward curvature. It suggests that Na is also loaded on SiO_2 support. I_{Na} profile in Fig. 2 shows a saturation curve. In contrast to Na on Pt particles, the Na on SiO_2 surface is suggested to grow to form the larger islands by increasing Na loading. The most probable growth mode of Na/Pt/SiO_2 catalyst surface as a function of the Na amount is illustrated in Fig. 3. The binding energies of Na 1*s* in the catalysts were observed in the range 1073.4 ~ 1073.8 eV, which suggests that the Na atoms are in a Na^+ state like Na_2O (*21*).

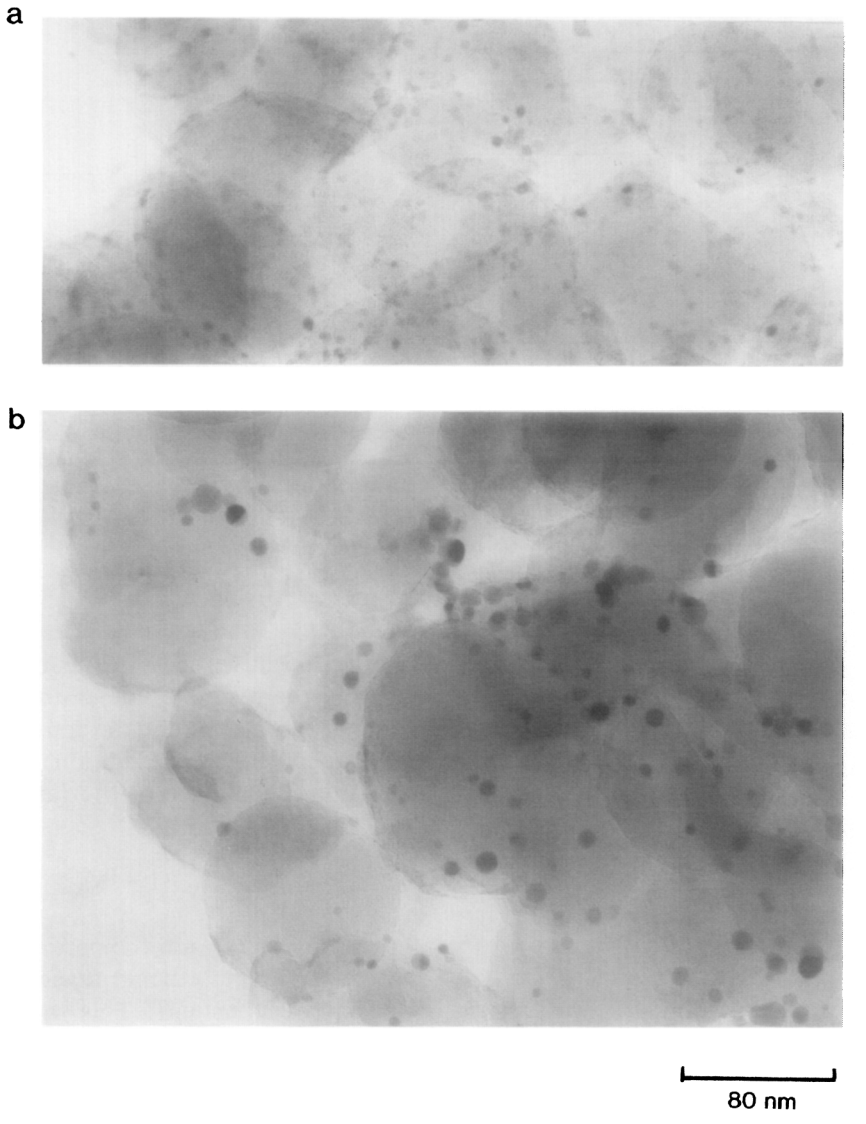

FIG. 1. TEM photographs of the catalysts. (a) Pt/SiO_2 ($\chi = 0.00$), (b) $Na/Pt/SiO_2$ ($\chi = 0.60$).

(*ii*) *Effects of Na Additives on Hydrogenation Rate and Activation Energy*

The activities and activation energies of ethene deuterogenation are listed in Table 3. In the presence of sodium, the rate of ethane formation became about four times higher as compared with that on the unpromoted catalyst. The activation energy (41 kJ $\cdot$ mol^{-1}) was a little higher than that of Pt/SiO_2 catalyst (33 kJ $\cdot$ mol^{-1}). As for $Na/Pt/SiO_2$, the rate increased with an increase of the sodium loading, while the activation energy was kept constant. The Pt on SiO_2 might have been depressed by acidic impurities on the support and in this case the role of Na additives would be to neutralize the acidic sites. However, the XP spectra revealed neither Cl peaks nor impurity peaks. The enhancement of the rate by Na addition

TABLE 2

The Binding Energies and Intensities of Pt $4f_{7/2}$ peaks in XP Spectra of the Catalysts

χ[a]	Pt $4f_{7/2}$ (eV)	Intensity[b]
0.00	70.53	0.19
0.16	70.38	0.12
0.43	70.28	0.07
0.60	70.14	0.07
0.70	70.08	0.07
0.86	70.02	0.07

[a] χ = Na/(Na + Pt).
[b] Arbitrary unit (normalized by the intensity of Si 2*s*).

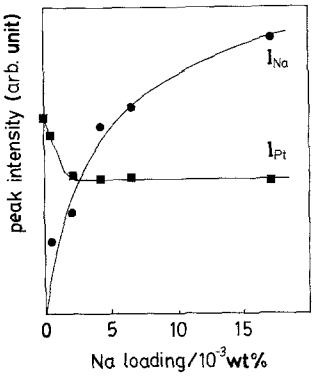

FIG. 2. Peak intensities of Pt $4f_{7/2}$ and Na 1*s* as a function of Na loading. Each peak was integrated and normalized by that of Si 2*p* of the sample. Pt $4f_{7/2}$ was corrected by H/*M* to avoid the decrease of surface area due to enlarging of particle size and to deduce the coverage of Na.

may be due to direct and indirect electronic transfer from Na_2O to Pt particles as discussed later, although there might be a minor effect by some acidic impurity. It is known that the rate-determining step of ethene hydrogenation on group VIII metals at lower temperatures is hydrogen dissociation and the apparent activation energy is positive. At higher temperatures the rate-determining step shifts to the second-hydrogen addition and the apparent activation energy is often negative (*22*). In our case of Na/Pt/SiO_2, the reaction temperatures are low enough (208–312 K) and the activation energies are positive. In addition, the partial pressure dependence of the rate was well fitted to (*23*)

$$r = k_{D_2} \times P_{D_2}/(1 + K_E \times P_E),$$

where P_{D_2} and P_E are the partial pressures of deuterium and ethene, respectively. k_{D_2} and K_E are constants. This rate equation implies a relatively strong adsorption of ethene and the rate-determining deuterium dissociation. This is confirmed by the fact that the rate data for ethene deuterogenation and hydrogen exchange had almost equal Arrhenius parameters as shown in Table 3. The rate of HD formation in H_2–D_2 exchange reaction on Pt/SiO_2 under the deuterogenation conditions was much larger than the rate of ethane formation. Furthermore, the activation energy for HD formation on Pt/SiO_2 (19 kJ · mol^{-1}) was smaller than that for ethane formation (33 kJ · mol^{-1}). This difference suggests that there is a kind of site on Pt/SiO_2 that is active mainly for H_2–D_2 exchange reaction on Pt/SiO_2. In other words, there may be at least two kinds of

TABLE 3

Activities (*r*) and Activation Energies (*E*) of Ethene Deuterogenation and Exchange on the Catalysts with Different Sodium Loading

χ[a]	Ethane[b]		HD[c]	
	E/kJ · mol^{-1}	*r*	*E*/kJ · mol^{-1}	*r*
0.86	41	3.98	40	4.10
0.70	41	3.53	41	3.56
0.60	41	3.31	40	3.35
0.43	41	3.20	40	3.07
0.16	40[d]	1.22		
0.00	33	1.00	19	4.04

[a] χ = Na/(Na + Pt).
[b] $D_2 + CH_2{=}CH_2$ reaction at 273 K (P_{D_2} = 1.3 kPa, $P_{CH_2=CH_2}$ = 3.0 kPa).
[c] $D_2 + H_2 + CH_2{=}CH_2$ reaction at 273 K (P_{D_2} = P_{H_2} = 0.6 kPa, $P_{CH_2=CH_2}$: 3.0 kPa).
[d] $T \geq 250$ K.

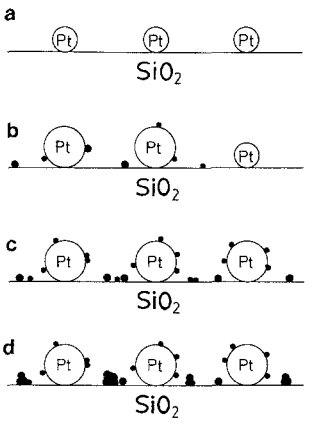

FIG. 3. Schematic models for $Na/Pt/SiO_2$ with various Na loading. (a) $\chi = 0.00$, (b) $\chi = 0.2$, (c) $\chi = 0.5$, (d) $\chi = 0.8$, $\chi = Na/(Na + Pt)$.

sites—one is active only for deuterium dissociation, where HD formation preferentially proceeds, and the other is the site on which deuterium and ethene react by the above equation. On $Na/Pt/SiO_2$, two kinds of sites with the different character do not exist because the activation energies and the preexponential factors were almost equal for ethane and HD formations. The increase of Pt particle size by Na addition may be related to this surface modification.

The Pt particle size and the Na coverage remained in the range of χ from 0.43 to 0.86, but ethane formation was enhanced by increasing Na loading. The extent of charge transfer from Na to platinum is roughly estimated from the shift of the binding energy of Pt $4f_{7/2}$ of $Na/Pt/SiO_2$. The more negative the charge of platinum was, the more rapidly the ethane formation proceeded. The electron transfer from sodium to platinum on SiO_2 surface is ascribed to a direct interaction between them and an indirect interaction through the support, as illustrated in Fig. 3.

A break was observed at ca. 250 K in the Arrhenius plot for $Na/Pt/SiO_2$ ($\chi = 0.16$). The activation energy in the lower temperature region was 32 kJ · mol^{-1} and in the higher temperature region was 40 kJ · mol^{-1}. These values are similar to those for Pt/SiO_2 and $Na/Pt/SiO_2$ ($\chi \geq 0.43$), respectively. This result for $Na/Pt/SiO_2$ ($\chi = 0.16$) also indicates a mixed state of the Pt particles with and without Na, as illustrated in Fig. 3.

Ethene hydrogenation has been regarded as structure insensitive as usual. In fact, there was no large difference between two Pt/SiO_2 catalysts with different dispersions, $H/M = 0.67$ and 0.014 in the hydrogenation. The rate of ethene formation per surface Pt atom on the $H/M = 0.014$ catalyst was more than 80% of that for the catalyst with $H/M = 0.67$. The activation energy was also unchanged. It is unlikely that the enhancement of these parameters by Na addition comes from the particle size enlargement.

(iii) *Isotope Distributions in the Products*

Table 4 summarizes the percentage distributions of d_i-ethane ($i = 1, 2, \cdots, 6$) at the initial stage of ethene deuterogenation on the catalysts with various Na loading. The amounts of deuterium atom incorporated in ethane molecule ($\Sigma i d_i / 6\Sigma d_i$) also listed in Table 4. $\Sigma i d_i / 6\Sigma d_i$ increased from 0.31 to 0.38 in the presence of Na, whereas it was almost independent of the amount of Na. The increase of $\Sigma i d_i / 6\Sigma d_i$ for the promoted catalyst may be caused by the increase of deuterium adsorption comparing to ethene and/or the

TABLE 4

The Percentage Distribution of *d*-Ethane at the Initial Stage of $D_2 + CH_2{=}CH_2$ Reaction at 263 K[a]

Ethane	χ = Na/(Na + Pt)					
	0.0	0.16	0.43	0.60	0.70	0.86
d_0	10	8	7	9	10	13
d_1	24	15	19	19	16	15
d_2	45	38	34	36	37	36
d_3	13	21	21	20	18	15
d_4	8	19	19	13	12	12
d_5	0	0	0	3	7	9
d_6	0	0	0	0	0	0
$100\Sigma i d_i / 6\Sigma d_i$	31	38	38	36	38	38

[a] $P_{D_2} = P_{CH_2=CH_2} = 1.3$ kPa.

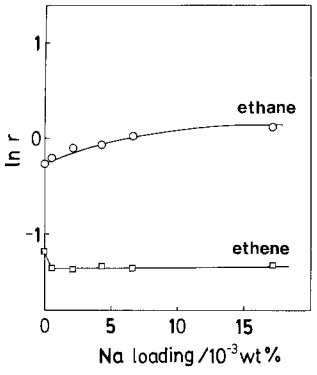

FIG. 4. The initial rates for ethane formation and ethene exchange. $P_{D_2} = P_{CH_2=CH_2} = 1.3$ kPa; the reaction temperature, 250 K.

equilibrium between associatively adsorbed ethane and half-hydrogenated intermediates shifted, these changes leading to the change of H/D ratio at the surface.

In our previous report for SMSI catalysts (*16*), it was demonstrated that there are site I (bare metal site) and site II (periphery site) and H/D ratios at the surface are different between these sites. On these surfaces with two different sites d_i-ethane should be produced in the order, d_0, $d_2 > d_1$ on the whole surface. It was illustrated that ethene isotopes were produced on site I or site II alone, in the order $d_2 > d_1 > d_0$ or $d_0 > d_1 > d2$, respectively (*16*). In the case of Na-promoted Pt/SiO_2 catalysts, the order is $d_2 > d_1 > d_0$ and there is no evidence of the H/D heterogeneity for ethane formation.

(*iv*) *Active Sites and Intermediates for Hydrogenation and Hydrogen Exchange*

The rates of ethene deuterogenation and hydrogen exchange in $D_2 + CH_2=CH_2$ system as a function of Na loading are shown in Fig. 4. The products in the hydrogen exchange reaction were d_1-ethene (C_2H_3D) and d_2-ethene ($C_2H_2D_2$). d_3- and d_4-ethene were negligible and below our detection limit in the initial stage of the reaction. The exchange rate is defined as an amount of deuterium atom in d_i-ethene (Σid_i) produced per unit time, while the deuterogenation rate is the sum of the formation rate of deuterogenated ethanes. The deuterogenation rate increased with an increase of the amount of Na while the exchange rate was almost constant except $\chi = 0.00$. Thus the rate of ethane formation seems to have a correlation with the binding energy of Pt $4f_{7/2}$, while the rate of exchange reaction correlates with the Na coverage on Pt surface. These results suggest that deuteroethene is formed at the neighboring sites of Na_2O island (periphery site) and ethane is produced at the far sites (bare metal sites). The electronic modification should be large at the periphery sites, which might be located in the region of two or three atoms around Na because of the screening of platinum metal (*15*).

The XP spectra for Pt $4f_{7/2}$ could not distinguish the periphery sites from bare metal sites. This may be because the ratio of the periphery sites should be less than that of the bare metal sites considering the small coverage of Na (0.2) and the particle size is large enough.

Figure 5 shows IR spectra of adsorbed ethene in the C–H stretching region. Both adsorption and measurement were carried out at 293 K. Five peaks were observed for each catalyst in Fig. 5. Three higher-wavenumber peaks, 3078, 3025, and 2965 cm^{-1} for Pt/SiO_2 and 3078 ~ 9, 3025, and 2964 cm^{-1} for $Na/Pt/SiO_2$ are due to π-ethene. The largest peaks at 2888 ~ 2869 cm^{-1} are assigned to di-σ-ethene on Pt (*24*). The absorption band in 2803 cm^{-1} on Pt/SiO_2 has been attributed to the first overtone of the asymmetric CH_3 bending mode of ethylidyne (*24*). These peaks diminished rapidly when D_2 was added at 293 K, evolving deuterogenated ethenes and ethanes in gas phase. This means that the observed surface species can be the reaction intermediates for ethane formation and ethene–deuterium exchange. The position and relative intensity of the peaks for π-ethene were not affected by sodium addition. On the contrary, the band for di-σ-ethene shifted by 18 cm^{-1} ($\chi = 0.16$) ~ 24 cm^{-1} ($\chi = 0.86$) and the relative intensity to those of π-ethene

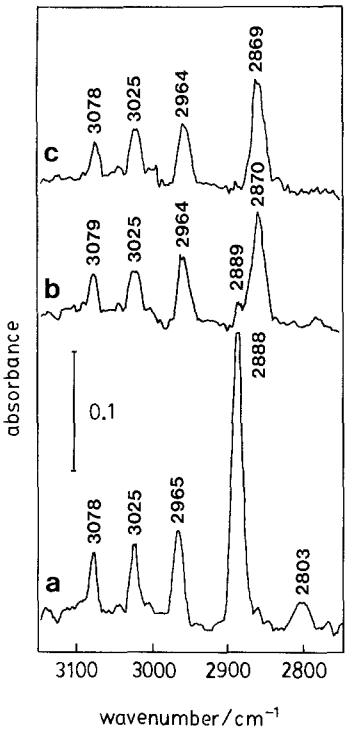

FIG. 5. IR spectra of C–H stretching region for ethene adsorbed on $Na/Pt/SiO_2$ catalysts; (a) $\chi = 0.00$ (Pt/SiO_2), (b) $\chi = 0.16$, (c) $\chi = 0.60$.

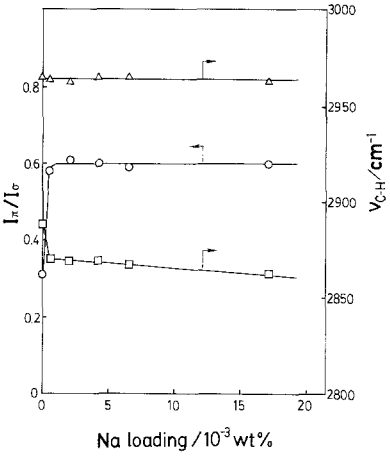

FIG. 6. The peak positions of C–H stretching for π-ethene (△) and di-σ-ethene (□) and the ratio of these peak intensities (I_π/I_σ, ○) as a function of Na loading.

became smaller than that of Pt/SiO_2. A small peak for di-σ-ethene was observed for the catalyst of $\chi = 0.16$ (2889 cm^{-1}), the position being the same as that for Pt/SiO_2. This supports the mixed state of pure Pt and Na-containing Pt particles in $Na/Pt/SiO_2$ ($\chi = 0.16$) as mentioned above.

The peak positions of π-ethene (around 2965 cm^{-1}) and for di-σ-ethene are plotted against the Na loading in Fig. 6. The ratio of the intensity of these two bands (I_π/I_σ) was also plotted as a function of Na loading in Fig. 6. The ratio, I_π/I_α, for $Na/Pt/SiO_2$ was much larger than that for Pt/SiO_2 and was almost independent of the Na loading. These results suggest that the π-ethene is located at the periphery sites, while the di-σ-ethene is formed on the bare sites as demonstrated in Fig. 7.

The constant peak position of π-ethene shows that the change in the electronic state characterized by Pt $4f_{7/2}$ XP spectra does not influence the electronic state of π-ethene, more precisely, C–H stretching. On the other hand, the C–H stretching of di-σ-ethene changed still after the saturation coverage of Na at 0.20, due to the further electronic effect from sodium supported on SiO_2 surface.

From the above discussion it is concluded that ethane is preferentially formed at the bare metal sites through the di-σ-intermediate, while ethene–deuterium exchange mainly proceeds at the periphery sites through the π-intermediate. The ratio of di-σ-ethene/π-ethene adsorbed on $Na/Pt/SiO_2$ decreased as compared with that on Pt/SiO_2 and the C–H

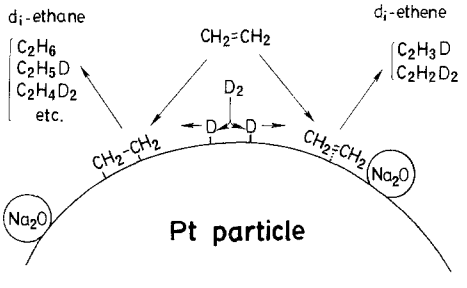

FIG. 7. A schematic model for short- and long-range promotion by Na additives in $D_2 + CH_2=CH_2$ reaction.

stretching frequency shifted toward lower wavenumber. Similarly to these observations, it has been reported that the adsorption of di-σ-ethene is weakened by the presence of alkali–metal on Pt(111) (*5*) and the negative charge moves from Pt to the adsorbed ethene (*23*). The electronic effect on the Pt surface is reflected in the increase of the activation energy for ethane formation. However, the rate of ethane formation increased with the Na-promoted Pt/SiO_2 catalysts due to the less adsorption of di-σ-ethene to lead to the enhancement of hydrogen dissociation, which competitively takes place as suggested by the rate equation. The C–H peak position of π-ethene and the rate of the ethene–deuterium exchange at the periphery sites were almost independent of the Na quantity. These results indicate the constant size of the Na on Pt particles over the whole range of Na loading.

REFERENCES

1. Imelik, B., Naccache, C., Condurier, G., Praliaud, H., Meriaudeau, P., Gallezot, P., Martin, G. A., and Vedrine, J. C., Eds. "Metal-Support and Metal-Additive Effects in Catalysis," Elsevier, Amsterdam, 1982.
2. Thomson, S. J., *J. Chem. Soc., Faraday Trans. 1* **83,** 1893 (1987).
3. Sinfelt, J. H., "Bimetallic Catalysts," Wiley, New York, 1984.
4. Zhou, X.-L., Zhu, X.-Y., and White, J. M., *Surf. Sci.* **193,** 387 (1988).
5. Windham, R. G., Bartram, M. E., and Koel, B. E., *J. Phys. Chem.* **92,** 2862 (1988).
6. Windham, R. G., and Koel, B. E., *J. Phys. Chem.* **94,** 1489 (1990).
7. Garfunkel, E. L., Maj, J. J., Frost, J. C., Farias, M. H., and Somorjai, G. A., *J. Phys. Chem.* **87,** 3629 (1983).
8. Crowell, J. E., Garfunkel, E. L., and Somorjai, G. A., *Surf. Sci.* **121,** 303 (1982).
9. Garfunkel, E. L., Crowell, J. E., and Somorjai, G. A., *J. Phys. Chem.* **86,** 310 (1982).
10. Kishinova, M., Pirug, G., and Bonzel, H. P., *Surf. Sci.* **140,** 1 (1984).
11. Kesraoui, S., Oukaci, R., and Blackmond, D. G., *J. Catal.* **105,** 432 (1987).
12. Ng, L., Uram, K. J., Xu, Z., Jones, P. L., and Yates, Jr., J. T., *J. Phys. Chem.* **86,** 6523 (1987).
13. Levin, M. E., Salmeron, M., Bell, A. T., and Somorjai, G. A., *J. Chem. Soc., Faraday Trans. 1* **83,** 2061 (1987).
14. MacLaren, J. M., Vvedensky, D. D., Pendry, J. B., and Joyner, R. W., *J. Chem. Soc., Faraday Trans 1* **83,** 1945 (1987).
15. Joyner, R. W., Pendry, J. B., Saldin, D. K., and Tennison, S. R., *Surf. Sci.* **95,** 1 (1984); MacLaren, J. M., Pendry, J. B., Joyner, R. W., and Meehan, P., *Surf. Sci.* **175,** 263 (1986).
16. Yoshitake, H., Asakura, K., and Iwasawa, Y., *J. Chem. Soc., Faraday Trans. 1* **84,** 4337 (1988).
17. Yoshitake, H., Asakura, K., and Iwasawa, Y., *J. Chem. Soc., Faraday Trans. 1* **85,** 2021 (1989).
18. Yoshitake, H., and Iwasawa, Y., *J. Catal.*, in press.
19. Perrichon, V., and Durupty, M. C., *Appl. Catal.* **42,** 217 (1988).
20. Anderson, R., "Structure of Metallic Catalysts," p. 361. Academic Press, New York, 1975.
21. Onishi, H., Egawa, C., Aruga, T., and Iwasawa, Y., *Surf. Sci.* **191,** 479 (1987).
22. Bond, G. C., "Catalysis by Metals." Academic Press, London, 1962.
23. Yoshitake, H., and Iwasawa, Y., in press.
24. Mohsin, S. B., Trenary, M., and Robota, H. J., *J. Phys. Chem.* **92,** 5229 (1988).